Integrated Pan-Cancer Analysis Reveals Distinct Clinical, Genomic and Immunological Features of the *LILRB* Immune Checkpoint Family in Acute Myeloid Leukemia

Zi-jun Xu
Affiliated People's Hospital of Jiangsu University
Xin-long Zhang
Affiliated Danyang Hospital of Nantong
Ye Jin
Affiliated People's Hospital of Jiangsu University
Shi-sen Wang
Affiliated People's Hospital of Jiangsu University
Yu Gu
Affiliated People's Hospital of Jiangsu University
Ji-chun Ma
Affiliated People's Hospital of Jiangsu University
Xiang-mei Wen
Affiliated People's Hospital of Jiangsu University
Jia-yan Leng
Affiliated People's Hospital of Jiangsu University
Zhen-wei Mao
Affiliated People's Hospital of Jiangsu University
Jiang Lin (linjiangmail@sina.com)
Affiliated People's Hospital of Jiangsu University https://orcid.org/0000-0002-4704-9157
Jun Qian
Affiliated People's Hospital of Jiangsu University

Research Article

Keywords: LILRBs, immune checkpoint genes, immune evasion, pan-cancer, leukemia

Posted Date: September 28th, 2021

DOI: https://doi.org/10.21203/rs.3.rs-810313/v1

Abstract

Background

Leukocyte immunoglobulin (Ig)-like receptor Bs (*LILRBs*), a family of type I transmembrane glycoproteins, are known to inhibit immune activation.

Methods

We comprehensively evaluated the transcriptional levels and prognostic significances of *LILRB* members in a broad spectrum of cancer types, focusing on its role in AML. In addition, we systematically characterized the genomic and immune landscape in AML patients with altered *LILRBs* expression.

Results

Here, we show that *LILRBs* were significantly dysregulated in a number of cancers, especially in acute myeloid leukemia (AML). Clinically, high expression of *LILRB1*-*LILRB4* predicted poor survival in six independent AML cohorts. Genetically, *LILRB1* was associated with more mutational events than other *LILRB* members, and multiple genes involving in immune activation were deleted in *LILRB1*-high patients. Epigenetically, *LILRB4* was significantly hypomethylated and marked by MLL-associated histone modifications in AML. Immunologically, *LILRBs* were positively associated with monocytic cells including M2 macrophages, but were negatively associated with tumor-suppressive CD8 T cells.

Conclusions

Our findings reveal critical immunological and clinical implications of *LILRBs* in AML, and indicate that *LILRBs* may represent promising targets for immunotherapy of AML.

Background

Acute myeloid leukemia (AML) is a highly fatal hematopoietic malignancy marked by various cytogenetic and molecular abnormalities and variable responses to treatment [1–3]. Currently, the mainstay of treatment for AML is cytotoxic chemotherapy [4], yet chemoresistance and relapse are commonly seen in in clinical practice. Some regimens under study, such as the combination of hypomethylating agents (HMAs) and Venetoclax, have shown promising results in certain subsets of AML patients [5, 6]. However, there remains an urgent need to develop novel effective therapies for various subsets of AML.

Noteworthy, immune checkpoint inhibitors (e.g., anti–PD-1 and anti–PD-L1 antibodies) have revolutionized cancer treatment during the past decade in treating cancers such as non–small-cell lung carcinoma and melanoma [7, 8]; however, the transfer of immunotherapy to AML has been less

successful than to other cancers [9]. Indeed, the AML microenvironment is predominantly immunosuppressive. For example, we have previously demonstrated that M2 macrophages, a classical immunosuppressive component, was preferentially enriched in AML than other hematological malignancies and normal controls [10]. Also, a recent single-cell RNA-seq study has reported proportionally fewer T cells and CTLs in AML than normal controls, and the function of these T cells are profoundly impaired, probably mediated by CD14 + monocyte-like cells [11, 12]. Moreover, Noviello et al. have reported that bone marrow T cells at AML relapse showed an exhausted phenotype, which was absent in patients maintaining long-term complete response [13]. These findings suggest encouraging therapeutic opportunities by modulating the immune environment in AML.

The leukocyte immunoglobulin (Ig)-like receptor subfamily B (*LILRB*) proteins are a group of type I transmembrane glycoproteins with extracellular Ig-like domains that bind ligands and intracellular immunoreceptor tyrosine-based inhibitory motifs (ITIMs) [14]. This group of receptors contains 5 members (*LILRB1*-*LILRB5*) that are mainly expressed in hematopoietic lineage cells and also various types of tumors [14]. As these proteins negatively regulate immune activation [15–17], they are often considered as immunosuppressive component in the tumor microenvironment (TME). In AML, the TME-modulating role of *LILRBs* have recently came into focus, especially for *LILRB4*. As demonstrated by the Gui group that *LILRB4* facilitates tissue infiltration of AML cells by substantially suppressing T cell activities, and blocking *LILRB4* activity efficiently inhibited AML development in vitro and in vivo [18, 19]. In addition, *LILRB1*, which showed predominant expression in monocytic AML cells as *LILRB4* did [20], was found to be up-regulated in dysfunctional CD8 + T cells from AML than T cells from healthy controls [21]. Interestingly, a non-immunological AML-promoting role was reported for *LILRB2*, which binds *Angptl2* to maintain stemness of normal stem cells and support leukemia development by inhibiting differentiation of AML cells [22]. Despite the functional importance of *LILRBs* in cancers, there currently lacked a systematic study to explore the expression patterns and clinical implications of all *LILRB* members in pan-cancers, especially in AML. Therefore, in this study, drawing on rich multi-omics data in the public domain, we comprehensively evaluated the transcriptional levels and prognostic significances of *LILRB* members in a broad spectrum of cancer types, focusing on its role in AML. In addition, we systematically characterized the genomic and immune landscape in AML patients with altered *LILRBs* expression.

Materials And Methods

Analysis of gene expression data

Briefly, the mRNA expression data of *LILRB* family in normal tissues were obtained from the Genotype-Tissue Expression (GTEx) project (www.gtexportal.org/) [23]. To confirm the expression patterns of *LILRBs* in normal tissues, we then explored the HPA (Human protein atlas) and FANTOM5 dataset from the human protein atlas database (http://www.proteinatlas.org/) [24]. Expression data of *LILRBs* for over 1000 cancer cell lines from various organ sites were accessed through Cancer Cell Line Encyclopedia (CCLE) (https://www.broadinstitute.org/ccle) [25]. Furthermore, RNA-seq data of 64 cell lines from The

Human Protein Atlas (HPA) ((https://www.proteinatlas.org/) [24] were used to validate expression patterns of *LILRBs* in cancer cell lines.

To determine the expression patterns of *LILRBs* between tumor and adjacent normal tissues across a broad range of cancer types, we systematically analyzed the gene expression data of 9465 tumor and 7831 normal samples based on RNA sequencing data from the TCGA and the GTEx projects. All these datasets were downloaded from the UCSC Xena project and were normalized between arrays using the limma package [26]. To validate the differential expression of *LILRBs* between AML and normal controls, we further retrieved two datasets containing both healthy and AML samples from Gene Expression Omnibus (GEO) (https://www.ncbi.nlm.nih.gov/geo/) (accession number GSE63270 and GSE30029). We also used a gene-expression dataset of normal hematopoietic cells (GSE42519) to assess the expression patterns of *LILRB* family genes at various stages of normal hematopoiesis.

We used the Hemap dataset curated by Dufva et al. [27], which includes datasets of AML, pre-B-ALL, DLBCL, and MM, to analyze the association between *LILRBs* expression and common molecular subtypes. The molecular subtypes were defined as previously described [27]. Three datasets-BeatAML, TCGA, and GSE13159-which have detailed cytogenetic information, were used to determine whether *LILRB4* expression was associated with MLL-rearranged AML. The counts per million (CPM) table of BeatAML were downloaded from the Supplementary Materials from Tyner et al. [28]. *LILRB4* expression level were log2 (1 + CPM) transformed before visualization. We computed single-sample GSEA (ssGSEA) enrichment scores for four MLL-r-related gene signatures from MSigDB (http://www.gsea-msigdb.org/gsea/msigdb/) using the R 'GSVA' package.

Analysis of AML single-cell RNA-sequencing (scRNA-seq) data

For single cell RNA-seq (scRNA) data analysis, previously published scRNA-seq data from 16 AML samples at diagnosis consisting of 30,712 bone marrow (BM) cells (Van Galen AML scRNA) were downloaded from GEO (GSE116256) [11], another scRNA-seq data for 8 patients consisting of 30,579 AML BM cells (FIMM AML scRNA) were retrieved via the Synapse Web Portal (https://www.synapse.org and doi: 10.7303/syn21991014). Data was processed and visualized using custom scripts provided by Dufva et al. [27].

Analysis of genetic alteration data

The genetic alterations of *LILRBs* from TCGA PanCancer Atlas studies (10967 patients), including somatic mutations, amplification, and deep deletion were assessed through the cbioportal for Cancer Genomics (http://www.cbioportal.org). To determine the association between *LILRBs* expression and common gene mutations, patients from the TCGA LAML cohort were first stratified into two groups by the median expression value of respective member genes, then mutation status for 24 most frequently mutated genes were identified using TCGA mutational data. The relationships between mutation status and *LILRBs* expression were analyzed by two-sided Fisher exact tests. The mutational profiles of patients

with high or low *LILRB1*/*LILRB5* expression were displayed as co-bar plots using the “Maftools” package [29]. To detect copy number alterations (deletions and amplications) in high- and low-*LILRB1* expressers, we analyzed filtered segmented copy number data in each group (Affymetrix SNP 6.0 platform) using the GISTIC 2.0 algorithm [30].

Analysis of gene methylation data

For comparison of methylation status of *LILRBs* between tumor and normal samples, beta values of Illumina 450k probes at the promoter region of five genes were retrieved by DiseaseMeth version 2.0 web portal (http://bio-bigdata.hrbmu.edu.cn/diseasemeth/analyze.html). Correlation between *LILRBs* methylation with expression and survival data across cancers were analyzed through the GSCALite platform [31]. For AML, the DiseaseMeth dataset contains methylation data of 271 AML (from TCGA, GSE62303, and GSE64934) and 10 normal samples (from GSE58477). Another methylation dataset-GSE63409-contains DNA methylation profiles of 20 leukemia stem cells, 24 blast cells and 30 normal hematopoietic stem and progenitor cells. Beta values of Illumina 450k probes nearest the transcription start site of the genes were selected to represent methylation level of the gene promoter area. Heatmaps displaying methylation levels of *LILRBs* across samples were generated using ‘pheatmap’ package.

Analysis of Chromatin immunoprecipitation-sequencing (ChIP-seq) data

ChIP-seq data for MLL-fusion proteins and three histone marks (H3K79me2, H3K27ac, and H3K4me3) from MV4-11 and THP-1 cells were obtained from GSE79899 [32]. For validation purpose, the three epigenetic marks from five other ChIP-seq datasets (H3K79me2 from GSE82116 and GSE71779; H3K27ac from GSE89336 and GSE71776; H3K4me3 from GSE61785 and GSE82116) were also included in our analyses. The gene tracks were generated by uploading the wiggle files as custom tracks onto the UCSC Genome Browser, assembly hg19. Wiggle files that have failed to be loaded as custom tracks were first converted to bigwig using the UCSC wigToBigWig tool.

Survival Analysis

We used the “Gene Outcome” module of TIMER2.0 (http://timer.cistrome.org/) [33] to investigate the association between the expression of *LILRB* members and clinical outcomes across 33 cancer types. The association between transcript levels of *LILRB* members and overall survival (OS) across cancers were assessed by univariate Cox regression. To confirm the prognostic value of *LILRBs* in AML, we further obtained five independent GEO datasets (GSE10358, n = 304; GSE37642 [U133A], n = 422; GSE37642 [U133plus2], n = 140; GSE106291, n = 250; GSE71014, n = 104) with available survival information. AML patients from these datasets and the TCGA dataset were divided into those with high and low gene expression, according to the optimal cut-off determined by the X-tile method [34]. We then performed Kaplan-Meier analysis (log-rank test) to compare the survival differences of two groups regarding overall survival (six datasets) and event-free survival (EFS) (only in TCGA dataset).

Immune response analysis

The relative abundances of 22 immune cell populations in AML patients were estimated using the CIBERSORT algorithm as previously described [10]. As CIBERSORT may not be suitable for the use of the RNA-seq data [35], this algorithm was exclusively applied to the TCGA LAML microarray dataset. For validation purpose, the relative fractions of immune cells were also estimated in two relatively large GEO datasets: GSE10358 and GSE6891. In addition, we used other deconvolution methods to quantify the proportions of monocytes (quanTIseq, MCP-counter, CIBERSORT abs, and xCell) and CD8 T cells (EPIC, TIMER, quanTIseq, MCP-counter, CIBERSORT abs, and xCell). These methods have been integrated as a unified interface by Sturm et al. [36] and are freely available through the TIMER 2.0 web portal (http://timer.comp-genomics.org/).

We evaluated the relationship between *LILRBs* and several notable immune checkpoint genes describe by De Simone et al. [37]. Spearman correlation analysis was used to test the association between *LILRBs* expression and these parameter estimates.

Differential gene expression analysis and functional enrichment analysis

Differential gene expression analysis for RNA sequencing data was performed using the raw read counts with the R/Bioconductor package “DESeq2”, controlled for the false discovery rate (FDR) by the Benjamini–Hochberg procedure. Gene Ontology (GO) analysis and Kyoto Encyclopedia of Genes and Genomes (KEGG) pathway analysis of *LILRB1*-coexpressed genes were performed using the STRING database (http://www.string-db.org/). GO and KEGG terms with false discovery rate (FDR)-corrected p values less than 0.05 were considered as significantly enriched. For displaying purposes, the top 10 GO terms of each three GO categories—biological process (BP), cellular component (CC), and molecular function (MF), and the top 10 KEGG pathway terms were visualized as bar plots.

Protein-protein interaction (PPI) network analysis

We applied STRING (http://string.embl.de/) to construct a protein-protein interaction (PPI) network of the differentially expressed genes (DEGs). We chose a confidence score > 0.9 as the judgment criterion. Cytoscape visualization software (version 3.6.1) was used to present the *LILRB1*-related sub-network.

Gene Set Enrichment Analysis (GSEA)

Gene set enrichment analysis (GSEA) was performed on the TCGA dataset using GSEA v4.1.0 software (http://www.broad.mit.edu/gsea). Statistical significance of GSEA results was determined by 1,000 gene set permutations, with signal-to-noise gene ranking. All the gene sets used in this study were obtained from GSEA MSigDB website (http://software.broadinstitute.org/gsea/msigdb/index.jsp), and the gene sets were considered to be significantly enriched at a false discovery rate < 0.25 and normalized P-value < 0.05. Three categories of gene sets were used in this study: C2, curated gene sets containing genes coregulated in response to specific perturbations; C7, immunologic signature gene sets that represent cell states and perturbations within the immune system; and H, hallmark gene sets which represent well-defined biological states or processes.

Statistical analysis and visualization

Wilcoxon rank sum tests were used to compare differences between two groups. Specifically, for Fig. 6a, we determined differential expression of *LILRBs* between each molecular subtype and the remaining samples for each disease subtype. The average fold changes (FCs) and Bonferroni-adjusted p-values (false discovery rate [FDR]) were computed using Wilcoxon rank sum tests. The FDR values were then combined for each *LILRB* members using Stouffer's method and categorized into five groups based on significance cutoffs for visualization (0.05, 0.01, 0.001, 1e-5, 1e-16). All statistical analyses and visualizations were performed using either indicated web servers or R version 4.0.4. Specifically, the expression map of *LILRBs* was generated using the "gganatogram" package [38], the box, bar, scatter and bubble plots were produced with the R package "ggplot2", "ggpubr" and "ggsci", the volcano plots were generated using the "EnhancedVolcano" package, and survival curves were made using the "survival" package. The correlation matrix was calculated and visualized using the "corrplot" or "ggcor" library. Finally, "circlize" was used to create the chord diagrams. All statistical tests were two-sided with p-values less than 0.05 considered significant.

Results

Expression patterns of LILRBs in normal tissues and cancer cell lines

In our first attempt, the expression patterns of *LILRBs* in different human tissues were determined based on RPKM values using GTEx [39] (http://www.GTExportal.org/home/). We note that the highest expression of *LILIBs* were observed in spleen, followed by blood and the lung tissue, while in other tissues, they were only weakly expressed (Fig. 1a and Supplementary Figure S1). Importantly, the preferential enrichment of *LILRBs* in spleen was further validated in the FANTOM5 and HPA (Human protein atlas) dataset (Supplementary Figure S2 and S3). Next, we explored the expression profiles of *LILRBs* in cancer cell lines from Cancer Cell Line Encyclopedia (CCLE). As shown in Fig. 1b and Supplementary Figure S4, *LILRBs* showed relatively high expression in cell lines of malignant hematological cell lines, such as acute myeloid leukemia (AML), acute lymphocytic leukemia (ALL), lymphomas, and multiple myeloma (MM). We also analyzed the expression levels of *LILRBs* based on RNA-seq in 64 different cell lines, as part of the Cell Atlas in the HPA. This analysis confirmed that *LILRBs* was highly expressed in cell lines of the myeloid and lymphocytic origin (Supplementary Figure S5). Notably, *LILRB1* and 2 showed higher expression in monocytes and the THP1 monocyte cell line. Together, these findings indicated a cellular-, tissue-, and disease- specificity of *LILRBs* expression.

Analysis of LILRB family gene expression levels in tumor and non-tumor tissues

Previous studies revealed that members of the *LILRB* family were upregulated in a number of cancers [40, 41]. Here, using pan-cancer datasets from the TCGA project, we found that the expression levels of *LILRB1-LILRB5* were positively correlated with each other (Fig. 1c), suggesting they may share some common features or functions; of them *LILRB5* showed relatively weak correlation with the other four genes. Combining the normal tissue of the GTEx dataset as controls, we then systematically compared *LILRBs* expression between tumor and adjacent normal tissue across 28 cancer types (9465 tumor and 7831 normal samples). Surprisingly, *LILRBs* were significantly dysregulated in almost all cancer types (Fig. 1d and Supplementary Figure S6). For *LILRB1*, *LILRB2*, and *LILRB4*, increased expression in tumors was more commonly seen; whereas *LILRB3* and *LILRB5* were significantly down-regulated in the majority of cancer types (Fig. 1d and e). For *LILRB1-LILRB4*, the most remarkable difference was observed between AML and normal its normal counterparts (Fig. 1d and Supplementary Figure S6). We also found that *LILRB1-LIRB4* were highly expressed in glioblastoma multiforme (GBM),head and neck squamous cell carcinoma (HNSC), kidney renal clear cell carcinoma (KIRC), kidney renal papillary cell carcinoma (KIRP), pancreatic adenocarcinoma (PAAD), and skin cutaneous melanoma (SKCM), whereas they were markedly decreased in adrenocortical carcinoma (ACC), lung adenocarcinoma (LUAD), lung squamous cell carcinoma (LUSC), and thymoma (THYM), as compared with normal controls (Fig. 1d and Supplementary Figure S6).

LILRBs were significantly up-regulated in AML and dynamically expressed during normal hematopoiesis

Our observations, together with previous findings [18], reflect an AML-specific expression patterns of *LILRBs*. We thus further explored the differential expression of *LILRBs* in two independent AML datasets with normal controls available. For these two datasets, only *LILRB1* and *LILRB3* were consistently up-regulated in AML (Fig. 1f and g), whereas *LILRB5* was down-regulated (Supplementary Figure S7a and b). Interestingly, *LILRB4*, which was previous shown to be increased in AML [18], exhibited no difference in expression in the two datasets (Fig. 1f and g).

We next sought to determine the expression patterns of *LILRBs* during normal hematopoiesis using a published data (GSE42519) [42]. We found that the transcripts of *LILRBs* was relatively high in bone marrow (BM) hematopoietic stem cells (HSCs), with a gradual diminishment when HSC differentiated to committed myeloid progenitors. The expression remained low in megakaryocyte-erythroid progenitor (MEP) and then steadily increased during myeloid maturation, reaching the highest level of expression in the mature polymorphonuclear cell (PMN) (Figure S7c). This dynamic regulation of *LILRBs* transcripts suggests a potential role of *LILRBs* in HSC biology.

Landscape of genetic alterations of LILRBs in tumors

We also investigated genetic alterations (including mutations, amplifications, and deletions) frequencies of *LILRBs* across pan-cancers. The average alteration frequencies of five genes were summarized in Fig. 4a and the oncoprint was present in Supplementary Figure S8a. The highest mutation loads of *LILRBs* was observed in SKCM (31.53%), followed by uterine corpus endometrial carcinoma (UCEC)

(14.56%), LUAD (14.49%), and LUSC (13.14%) (Fig. 4a and c). Overall, *LILRB1* was the most highly mutated and *LILRB3* the least; the most frequent genomic variants were missense mutations for five genes (Fig. 4b and Supplementary Figure S8b). For diffuse large B-Cell lymphoma (DLBC), mesothelioma (MESO), and THYM, copy number alterations (CNAs) were the only genetic events (Fig. 4a). Amplifications were more commonly seen in cancers such as ACC, uterine carcinosarcoma (UCS), and bladder urothelial carcinoma (BLCA), while deletions were mostly found in cancers like brain lower grade glioma (LGG), ovarian serous cystadenocarcinoma (OV), and testicular germ cell tumor (TGCT) (Fig. 4a and d). In AML where *LILRBs* expression were markedly changed, however, genetic alteration frequencies of these genes were extremely low, suggesting other mechanisms might contribute to the abnormal *LILRBs* expression in AML (Fig. 4a, c, and d).

LILRBs were hypomethylated in AML

We next asked whether DNA methylation regulates the expression of *LILRBs* in cancers. We first retrieved the methylome data of *LILRBs* across 30 cancer types with matched controls through the human disease methylation database Diseasemeth version 2.0 (http://bio-bigdata.hrbmu.edu.cn/diseasemeth/). Surprisingly, we found that *LILRB* members were significantly hypomethylated in almost all cancer types analyzed as compared to normal samples (Fig. 3a). We then investigated the correlation between methylation and expression levels of *LILRBs* using GSCALite [31]. We found that methylation level of *LILRB1* was negatively associated with its mRNA expression in most cancer types (Fig. 3b). For other *LILRB* members, methylation and expression levels were also mainly negatively correlated, with only a few positive correlations (Fig. 3b). Importantly, consistent with the increased expression of *LILRBs* in AML, significantly hypomethylated promoters of *LILRBs* were observed in both the Diseasemeth (AML, n = 271; normal, n = 10) and GSE63409 dataset (AML, n = 44; normal, n = 30) (Fig. 3c and d). We then studied the correlation between promoter methylation and expression of *LILRBs* in TCGA AML dataset. Interestingly, expression of *LILRB2*, *LILRB3*, and *LILRB4* correlated negatively with promoter methylation and the most significant correlation was observed for *LILRB4* (Fig. 3b and e). This observation is consistent with a previous report that decitabine (DAC, a demethylating agent) treatment with AML cells remarkably promoted expression of *LILRB* family members, especially *LILRB4* [43]. Collectively, these results suggest that DNA hypomethylation might contribute to the activation of *LILRB* members in AML. Further, analyzing the relation between methylation and survival revealed that hypomethylation of *LILRBs* predicted worse survival in most cancers (Fig. 3f). In AML, hypomethylation of *LILRB4* was associated with adverse outcome and hypomethylation of *LILRB5* with favorable outcome (Fig. 3f).

Adverse prognostic impact of LILRBs in AML

Next, we used Cox regression analyses to explore the association between *LILRBs* expression and overall survival (OS) in TCGA pan-cancer datasets. Overall, we found the significance and direction of the prognostic significances varied, depending on the cancer types analyzed. For example, increased expression of *LILRB* family members were generally associated with worse OS in KIRC, LAML, LGG, TGCT, THYM, and uveal melanoma (UVM). While in SKCM and metastatic SKCM, the reverse was observed

(Fig. 4a). Interestingly, a previous study has also performed Cox analyses in TCGA data, showing that *LILRB1-LILRB4* negatively impacts the survival of AML patients. It is of particular interest to validate the prognostic value of *LILRBs* using Kaplan-Meier methods in larger patient cohorts of AML. To this end, we collected five independent datasets from GEO; X-tile was used to determine the optimal thresholds for each *LILRB* members in TCGA and GEO datasets. First, we were able to validate the adverse prognostic impact for *LILRB1-LILRB4* in the TCGA cohorts (Fig. 4b), whereas high *LILRB5* was associated with favorable outcome (Supplementary Figure S9). Importantly, the prognostic value of *LILRB1-LILRB4* also extended to the event-free survival (EFS) endpoint and cytogenetically normal (CN)-AML subsets (Supplementary Figure S10a-c). Furthermore, the adverse prognostic impact of *LILRBs* was validated in TCGA microarray data (n = 183) (Supplementary Figure S10d) and other five independent cohorts of AML patients (GSE10358, n = 304; GSE37642 [U133A], n = 422; GSE37642 [U133plus2], n = 140; GSE106291, n = 250; GSE71014, n = 104) (Fig. 5a-e), although in some cases only a trend for shorter OS was observed. For subsequent analyses, we will focus on the role of *LILRB1-LILRB5* in AML, due to frequent alterations and high prognostic values of *LILRBs* in this malignancy.

LILRB4 is aberrantly overexpressed in MLL-rearranged AML and may be a target of MLL fusion proteins

We next asked whether *LILRBs* expression could be associated with specific molecular subtypes in AML. To this end, we examined the expression differences of *LILRBs* across published transcriptomic subtypes in the Hemap dataset (including AML, pre-B-ALL, DLBCL, and MM) [27]. As expected, all five *LILRB* members were more highly expressed in monocyte-like AML, while their expressions were relatively weak in the other three malignancies (Fig. 6a). One unanticipated exception to this overall trend was the strong enrichment of *LILRB4* in MLL-rearranged AML (Monocyte – like – MLL) and ALL (KMT2A) (Fig. 6a). To confirm this observation, we subsequently analyzed the transcript levels of *LILRB4* in 15 leukemia cell lines with or without MLL-rearrangements from the CCLE database. Leukemia cell lines with presence of MLL-fusion genes exhibited markedly higher *LILRB4* expression than those lack MLL-fusion genes, whether *LILRB4* expression was detected by RNA-seq (Fig. 6b) or Affymetrix microarray (Supplementary Figure S11a). Accordingly, analysis of three large primary patient datasets (BeatAML, TCGA, and GSE13159) revealed consistently highest *LILRB4* expression in MLL-rearranged AML as compared to other cytogenetic/clinicopathologic leukemia entities (Fig. 6c, Supplementary Figure S11b and c). To further confirm the relevance of *LILRB4* expression in MLL-rearranged AML, we collected four MLL-rearrangement-related gene signatures from MSigDB and computed ssGSEA scores of these signatures for each sample in the TCGA dataset. Then, we compared the ssGSEA scores computed for high *LILRB4*-expressing samples with those in low *LILRB4*-expressing samples. We found gene-sets down-regulated in MLL-rearranged AML (MULLIGHAN_MLL_SIGNATURE_1_DN) showed significantly lower ssGSEA scores in *LILRB4*-high patients than in *LILRB4*-low patients; whereas for gene-sets up-regulated in MLL-rearranged AML (MULLIGHAN_MLL_SIGNATURE_1_UP), the opposite was seen (Fig. 6d). Also, the ssGSEA scores of two MLL-rearranged-governed signatures (ROSS_AML_WITH_MLL_FUSIONS and

VALK_AML_WITH_11Q23_REARRANGED) were significantly up-regulated in high *LILRB4* expressers (Supplementary Figure S11d).

It has been shown that target genes of MLL-fusions were often hypomethylated [44, 45], which is consistent with our previous observations. Also, promoters of these genes were often enriched with transcription activation-associated histone marks (H3K79me2, H3K27ac, and H3K4me3) [32]. To determine whether *LILRB4* expression could be directly regulated by MLL-fusion gene, we analyzed a published ChIP-seq dataset (GSE79899) of MLL-fusion proteins, H3K79me2, H3K27ac, and H3K4me3 for MV4-11 (MLL-AF4) and THP-1 (MLL-AF9) cell lines. We found a significant enrichment of MLL-N proteins in the promoter regions of *LILRB4* gene for both cell lines, while punctuated binding peaks of H3K79me2, H3K27ac, and H3K4me3 were observed in both the promoter and gene body of *LILRB4* (Fig. 6e). Importantly, a similar enrichment of the three epigenetic marks was seen in five other ChIP-seq datasets (H3K79me2 from GSE82116 and GSE71779; H3K27ac from GSE89336 and GSE71776; H3K4me3 from GSE61785 and GSE82116) (Fig. 6f). Overall, these results suggest that MLL fusion proteins may be a direct regulator of *LILRB4* expression.

LILRB1 expression correlates with distinct genomic alterations in AML

We then examined the associations between *LILRBs* expression and the clinical and genetic characteristics in the TCGA AML cohort. We found an association between *LILRBs* expression and the French-American-British (FAB) classification of AML: a higher percentage of myelomonocytic or monocytic morphology (M4/M5 subtypes) and a lower percentage of FAB M2/M3 was observed in patients with high *LILRBs* expression (Fig. 7a). Moreover, high *LILRBs* expressers were more likely to be > 60-year-old and less likely to present with favorable cytogenetics (Fig. 7a).

To determine whether *LILRB1-LILRB5* correlated with distinct mutational profiles characterized for AML, we identified significantly mutated genes occurred in patients with high and low *LILRB1-LILRB4* expression (as stratified by the median expression value of respective genes), using curated mutational data from TCGA. Overall, we found *LILRB1* and *LILRB5* expression was associated with more mutational events than the other three genes (Fig. 7b). As shown in Fig. 7c, patients with high *LILRB1* expression had higher frequency of mutations in *U2AF1* (7% vs 1%) and *RUNX1* (14% vs 4%), while *IDH1* (14% vs 4%) was more frequently mutated in those with low *LILRB1* expression. High *LILRB5* expression was positively correlated with *TP53* mutations and negatively correlated with *FLT3* and *WT1* mutations. For other three genes, *LILRB2* was associated with mutations in *IDH1* and *STAG2*, *LILRB3* with *WT1*, and *LILRB4* with *RUNX1* (Fig. 7b).

To further explore the association between *LILRBs* expression and copy number variation (CNV), we performed GISTIC2.0 analysis of TCGA copy number data and assessed copy number alterations between in two patient groups. We focused on *LILRB1*, as it was consistently dysregulated and showed the greatest mutational events in AML patients. Interestingly, *LILRB1*-low patients had no somatic copy number alterations (Supplementary Figure S12), whereas *LILRB1*-high patients had 14 significantly

deleted regions and four significantly amplified region (FDR = 0.25) (Fig. 7d). Interestingly, the majority of genes deleted in *LILRB1*-high patients were involved in inflammatory responses (including cytokines and genes essential for microbial killing and antigen processing and presentation, see Supplementary data 1 for detail). Also, a number of genes belongs to the cadherin (*CDH*) and protocadherin (*PCDH*) family, which often exerts tumor-suppressive functions [46], were significantly deleted. In contrast, *LILRB*-high AML patients had recurrent amplification at loci essential in AML pathogenesis, including *KMT2A* and *ERG* [47, 48] (Fig. 7d).

Correlations Between LILRBs and Tumor Immune Infiltrating Cells (TIICs) in AML

Considering that *LILRBs* might play important roles in the TME, we further explored the correlations between *LILRBs* and the level of immune cell infiltration in TCGA AML cohort. It is noteworthy that, among the 22 cell types, monocytes had the highest positive correlations with *LILRB1-LILRB4* (Fig. 8a), consistent with previous finding that *LILRBs* were preferentially expressed in monocytic AML [19, 49]. This monocytic preference was also confirmed in two recently published scRNA-seq datasets of AML (Van Galen AML scRNA, Fig. 8b and FIMM AML scRNA, Supplementary Figure S13a). Interestingly, *LILRB4* was exclusively correlated with M2 macrophages (Fig. 8a), a high immunosuppressive component in the TME. By contrast, *LILRB1-LIRB4* were negatively correlated with the infiltrating levels of tumor-suppressive immune cells, such as resting T cells CD4 memory cell, CD8 T cells, memory B cells, plasma cells, and resting NK cells (Fig. 8a). Similar results were found by analyzing the CIBERSORT estimates in the GSE10358 and GSE6891 dataset (Supplementary Figure S13b and c). Importantly, when other methods were used for calculating the relative fractions of TIICs, positive associations between *LIRB1-LILRB4* and monocytes were consistently seen, while negative associations between *LILRB1-LILRB4* and CD8 T cells were proved for most-if not all-methods in all three datasets (Supplementary Figure S13d-f). Further analysis of normal cell populations from the Hemap dataset revealed that *LILRBs* were highly expressed in myeloid lineage immune cells (monocytes, macrophages, dendric cells, myeloid progenitors, and neutrophils), with consistent low expression in T cells (CD4 + T cells and T/NK cells) (Fig. 8c). Collectively, these findings further confirmed the immunosuppressive roles of *LILRBs* in cancer TME.

Correlation between LILRBs and immune checkpoints in AML

Given that immune checkpoints have been proved to be promising therapeutic target for cancer treatment, we therefore evaluated the relationship between *LILRBs* and a collection of checkpoint genes describe by De Simone et al. [37]. Results from Spearman correlation analyses are given in Supplementary Data 2. As shown in the Circos plots, *LILRB1-LILRB3* all showed strong positive correlations with *CD86*, *VISTA*, and *HAVCR2* (Fig. 8d-f), indicating a possible synergistic effect between these genes. In contrast, no significant correlations were observed between *LILRB4*/5 and these

checkpoints (Supplementary Figure S14a and b). These results further highlight *LILRBs* potentially as major signaling pathways involved in immunosuppression in the AML microenvironment.

The biological significance of LILRBs expression in AML

We then sought to investigate the biological features associated with *LILRBs* in AML. Since the expression of five *LILRB* members were highly correlated, a comparison of gene expression profiles of patients with high and low *LILRB1* expression (as determined by the median expression value) was performed. Overall, 799 genes (490 up- and 309 downregulated; adjusted $p < 0.05$; $log2FC \leq -1.5$ or $log2FC \geq 1.5$) were differentially expressed in *LILRB1*^{high} versus *LILRB1*^{low} patients (Fig. 9a and Supplementary Data 3). Among the genes positively correlated with *LILRB1* were, as expected, the other members of the *LILRB* family (Fig. 9a). Also, genes associated with presence of monocytes/macrophages (*CD14*, *CD68*) or M2 macrophage polarization (*MSR1*, *MRC1*, *CD163*) were significantly up-regulated in high *LILRB1* expressers (Fig. 9a), in line with our previous findings. Next, we used STRING database to construct a protein-protein interaction (PPI) network of the differentially expressed genes (DEGs), with a confidence score > 0.90. Genes interacted with *LILRB1* and their sub-networks were shown through Cytoscape software (Fig. 9b). We found 12 genes directly interacting with *LILRB1*: *PILRA*, *TLR8*, *SIGLEC7*, *CD300C*, *FCGR2A*, *FCGR2B*, *FCGR3A*, *CD86*, *FGR*, *HCK*, *IL10*, *ITGAX*. Among them, *CD300C*, *FCGR2A*, *FCGR2B*, and *FCGR3A* also had connections with the other four *LILRB* members (Fig. 9b). GeneMANIA results also revealed that genes of the *FCGR* and *CD300* family were closely correlated with *LILRBs*. These genes were mainly involved in negative regulation of leukocyte mediated immunity and negative regulation of immune system process (Supplementary Figure S15a).

We then performed GO analysis using these DEGs and the top 10 significant terms of BP, MF and CC enrichment analysis were shown (Fig. 9c). Notably, in terms of BP, immune response-related processes were significantly enriched, such as inflammatory response, immune system process, and immune response. KEGG and Reactome Pathway analyses also revealed immune response pathways, including cytokine – cytokine receptor interaction, cytokine signaling in immune system, innate immune system, antigen processing – cross presentation, and adaptive immune system were mainly enriched (Fig. 11d and Supplementary Figure S15b).

Finally, GSEA was conducted in the *LILRB1*^{high} and *LILRB1*^{low} cohorts. For the C2 collection of curated gene sets from the MSigDB, the VALK_AML_CLUSTER_5 gene set (96% of the samples are FAB M4 or M5 subtype) was predominantly enriched in *LILRB1*^{high} group. Also enriched were gene sets of MLL-fusion and *NPM1*-mutation, two distinct entities often associated with monocytic features of AML (Fig. 10a). For the C7 immunologic collection, the *LILRB1*^{high} group had principal enrichment in genes up-regulated in monocytes compared to other immune cells (Fig. 10b), and multiple immune activities were enriched in the *LILRB1*^{high} group for HALLMARK gene sets (Fig. 10c).

Discussion

The *LILRB* family members-*LILRB1*-5-are a group of proteins containing the immune-inhibitory ITIM motifs which negatively regulate immune cell activation [14]. Here, using RNA-seq data of normal tissues from GTEx, FANTOM5, and HPA, we showed that *LILRB* members were predominantly enriched in the spleen, consistent with their immune modulatory functions. In cancer cell lines, *LILRBs* showed relatively high expression in cell lines of malignant hematological origin, in line with the selective expression of *LILRBs* in hematopoietic lineage cells. Indeed, abnormal expression of *LILRBs* has been documented in various cancers, such as lung cancer [50], hepatocellular carcinoma (HCC) [51], and certain types of subtypes of adenocarcinoma [41]. In this study, based on combined datasets from TCGA and GTEx, we comprehensively analyzed *LILRBs* expression between tumor and adjacent normal tissue across 28 cancer types (9465 tumor and 7831 normal samples). Our data showed that *LILRBs* were significantly dysregulated in the majority of tumor types. For *LILRB1-4*, the most striking difference was seen between AML and its normal counterparts. Although previous study has reported increased expression of *LILRB4* in AML [19, 49], this was not seen in two independent validation sets of AML patients, probably due to technical/biological heterogeneity across studies. However, we do note a strong enrichment for *LILRBs* in the monocytic lineage; this observation was confirmed in HPA pan-cancer cell lines dataset, single-cell transcriptomics of immune cells, immune cell abundances estimated using bulk TCGA samples, and GSEA analysis of monocyte-related gene sets, in agreement with previous reports [19, 20, 22, 49].

Despite being positively correlated with monocytes, *LILRB1-4* were negatively correlated with the density of CD8 + T and NK cells, which are considered essential for effective anti-tumor immunity [27]. It has been shown that activated *LILRB4* on monocytic AML cells recruits *SHP-2* and upregulates *NFκB*, leading to increased *ARG1* and *uPAR* accompanied by a concomitant suppression of T cell activity [18, 19]. This might provide a potential mechanistic explanation to our observations. It should be noted that bone marrow (BM)-T cells in AML are often functionally impaired [11–13, 52], possibly mediated by malignant monocyte-like cells from AML [11, 19, 21, 53]. Further research aimed to unravel the underlying molecular mechanisms is clearly warranted, as this may provide opportunities for identification of new drugs targets and therapeutics that can circumvent the T cell suppression state in AML.

Immunosuppressive factors, such as indoleamine 2,3-dioxygenase 1 (*IDO1*), *CD200*, and *TIM-3* were reported to be closely associated with a poor outcome in AML [54–56]. In a preliminary analysis, Deng et al. studied the prognostic relevance of several co-stimulating and co-inhibitory receptors in TCGA AML dataset, including *LILRB1-LILRB4* [19], but there is limited data and require validation in large datasets. Here, we independently validated the prognostic significances of *LILRB* members in five independent datasets. Strikingly, we showed that *LILRB1-4* adversely impacted survival in almost all analyzed datasets. Of interest, we also noticed that *LILRB4* was significantly associated with M2 macrophage abundances. This observation raises the possibility that *LILRB4* might contribute to leukemogenesis through M2 macrophages. Our group has recently reported that M2 macrophages fractions were selectively upregulated in AML than other four hematological malignancies and normal controls [10]. Importantly, we also demonstrated a superior predictive performance of the M2 marker *CD206* (*MRC1*) than classical prognosticators in AML. Interestingly, in this study we found that *CD206* was significantly up-regulated in high *LILRB1* expressers. As *CD206* + and/or *LILRB4* + monocytes could suppress T-cell

proliferation and create an immunosuppressive microenvironment in AML [19, 53], it could be hypothesized that at least part of the prognostic value of *LILRBs* could be attributed to the immune-suppressive TME it contributed. Acute monocytic leukemia often harbors mixed-lineage leukemia (MLL) rearrangements, an aggressive phenotype with limited treatment options and poor survival rates, which might also explain the observed result. Indeed, we demonstrated that *LILRB4* was aberrantly overexpressed in MLL-rearranged AML and might be a direct target of the MLL fusion proteins.

In a recent pan-hematological-malignancies study, the authors have found that *LILRB2* could distinguish lymphoma and leukemia subtypes with high immune infiltration from those harboring lower cytolytic score [27]. We consistently found multiple genes involving in immune activation (including cytokines and genes essential for microbial killing and antigen processing and presentation) were deleted in *LILRB1*-high patients, indicating a delicate balance between immune activation and suppression in the TME.

Indeed, an integrated analysis of transcriptomic and proteomic data has uncovered and ranked *LILRBs* among the top potential chimeric antigen receptor (CAR) targets in AML [57]. Preliminary evidence from the Gui group also suggests that blocking *LILRB4* activation effectively reversed T-cell suppression and inhibited AML cell infiltration [18]. Given that *LILRBs* are selectively dysregulated in AML, it is tempting to speculate that AML positive for these proteins might be good candidates for immunotherapy. Future cancer immunotherapy clinical trials will be critical to further validate these findings.

In this study, we provided a comprehensive analysis of the expression patterns and clinical significances of *LILRBs* across pan-cancers, focusing its role in AML. We also analyzed the association of *LILRBs* expression with genomic features and tumor immunity in AML. Our data revealed up-regulated expression of *LILRBs* in AML and that higher expression levels of these genes predicted worse outcome. In addition, *LILRBs* were associated with an immune-suppressive TME in AML. Overall, these findings suggest important immunological and clinical implications of *LILRBs* in AML, which warrants further clinical investigation with immunotherapy specifically targeting AML with *LILRBs* dysregulations.

Declarations

Acknowledgements

Not applicable.

Funding

This study was supported by National Natural Science foundation of China (81970118, 81900163), Medical Innovation Team of Jiangsu Province (CXTDB2017002), Zhenjiang Clinical Research Center of Hematology (SS2018009), Social Development Foundation of Zhenjiang (SH2019065, SH2019067), Scientific Research Project of The Fifth 169 Project of Zhenjiang (21).

Availability of data and materials

The datasets analyzed in this study are available in the following open access repositories:

GTEx, www.gtexportal.org/

HPA, https://www.proteinatlas.org/

CCLE, https://www.broadinstitute.org/ccle

TCGA, https://portal.gdc.cancer.gov/, http://www.cbioportal.org

GEO, https://www.ncbi.nlm.nih.gov/geo/ (GEO accession numbers: GSE63270, GSE30029, GSE42519, GSE13159, GSE116256, GSE63409, GSE79899, GSE82116, GSE71779, GSE89336, GSE71776, GSE61785, GSE10358, GSE37642, GSE106291, and GSE71014)

FIMM AML scRNA data, https://www.synapse.org (doi: 10.7303/syn21991014)

DiseaseMeth, http://bio-bigdata.hrbmu.edu.cn/diseasemeth/analyze.html

TIMER 2.0, http://timer.comp-genomics.org/

Author contributions

JQ, JL, and Z-WM conceived and designed the study; Z-JX, X-LZ, YJ, S-SW, and YG collected and assembled data; Z-JX, J-CM, X-MW, and J-YL performed data analysis; Z-JX drafted the manuscript; JQ, JL, and Z-WM participated in study supervision and commented on the manuscript. All authors read and approved the final manuscript.

Ethics approval and consent to participate

Not applicable.

Consent for publication

Not applicable.

Competing interests

The authors declare that they have no competing interests.

References

1. Löwenberg B, Downing JR, Burnett A: Acute myeloid leukemia. *N Engl J Med* 1999, 341(14):1051-1062.
2. Byrd JC, Mrózek K, Dodge RK, Carroll AJ, Edwards CG, Arthur DC *et al*: Pretreatment cytogenetic abnormalities are predictive of induction success, cumulative incidence of relapse, and overall

survival in adult patients with de novo acute myeloid leukemia: results from Cancer and Leukemia Group B (CALGB 8461). *Blood* 2002, 100(13):4325-4336.

3. Marcucci G, Mrózek K, Bloomfield CD: Molecular heterogeneity and prognostic biomarkers in adults with acute myeloid leukemia and normal cytogenetics. *Curr Opin Hematol* 2005, 12(1):68-75.
4. Döhner H, Estey EH, Amadori S, Appelbaum FR, Büchner T, Burnett AK *et al*: Diagnosis and management of acute myeloid leukemia in adults: recommendations from an international expert panel, on behalf of the European LeukemiaNet. *Blood* 2010, 115(3):453-474.
5. DiNardo CD, Pratz KW, Letai A, Jonas BA, Wei AH, Thirman M *et al*: Safety and preliminary efficacy of venetoclax with decitabine or azacitidine in elderly patients with previously untreated acute myeloid leukaemia: a non-randomised, open-label, phase 1b study. *Lancet Oncol* 2018, 19(2):216-228.
6. DiNardo CD, Maiti A, Rausch CR, Pemmaraju N, Naqvi K, Daver NG *et al*: 10-day decitabine with venetoclax for newly diagnosed intensive chemotherapy ineligible, and relapsed or refractory acute myeloid leukaemia: a single-centre, phase 2 trial. *Lancet Haematol* 2020, 7(10):e724-e736.
7. Topalian SL, Hodi FS, Brahmer JR, Gettinger SN, Smith DC, McDermott DF *et al*: Safety, activity, and immune correlates of anti-PD-1 antibody in cancer. *N Engl J Med* 2012, 366(26):2443-2454.
8. Brahmer JR, Tykodi SS, Chow LQ, Hwu WJ, Topalian SL, Hwu P *et al*: Safety and activity of anti-PD-L1 antibody in patients with advanced cancer. *N Engl J Med* 2012, 366(26):2455-2465.
9. Lichtenegger FS, Krupka C, Haubner S, Köhnke T, Subklewe M: Recent developments in immunotherapy of acute myeloid leukemia. *J Hematol Oncol* 2017, 10(1):142.
10. Xu ZJ, Gu Y, Wang CZ, Jin Y, Wen XM, Ma JC *et al*: The M2 macrophage marker CD206: a novel prognostic indicator for acute myeloid leukemia. *Oncoimmunology* 2020, 9(1):1683347.
11. van Galen P, Hovestadt V, Wadsworth Ii MH, Hughes TK, Griffin GK, Battaglia S *et al*: Single-Cell RNA-Seq Reveals AML Hierarchies Relevant to Disease Progression and Immunity. *Cell* 2019, 176(6):1265-1281.e1224.
12. Lamble AJ, Kosaka Y, Laderas T, Maffit A, Kaempf A, Brady LK *et al*: Reversible suppression of T cell function in the bone marrow microenvironment of acute myeloid leukemia. *Proc Natl Acad Sci U S A* 2020, 117(25):14331-14341.
13. Noviello M, Manfredi F, Ruggiero E, Perini T, Oliveira G, Cortesi F *et al*: Bone marrow central memory and memory stem T-cell exhaustion in AML patients relapsing after HSCT. *Nat Commun* 2019, 10(1):1065.
14. Kang X, Kim J, Deng M, John S, Chen H, Wu G *et al*: Inhibitory leukocyte immunoglobulin-like receptors: Immune checkpoint proteins and tumor sustaining factors. *Cell Cycle* 2016, 15(1):25-40.
15. Banchereau J, Zurawski S, Thompson-Snipes L, Blanck JP, Clayton S, Munk A *et al*: Immunoglobulin-like transcript receptors on human dermal CD14+ dendritic cells act as a CD8-antagonist to control cytotoxic T cell priming. *Proc Natl Acad Sci U S A* 2012, 109(46):18885-18890.
16. Baudhuin J, Migraine J, Faivre V, Loumagne L, Lukaszewicz AC, Payen D *et al*: Exocytosis acts as a modulator of the ILT4-mediated inhibition of neutrophil functions. *Proc Natl Acad Sci U S A* 2013, 110(44):17957-17962.

17. van der Touw W, Chen HM, Pan PY, Chen SH: LILRB receptor-mediated regulation of myeloid cell maturation and function. *Cancer Immunol Immunother* 2017, 66(8):1079-1087.
18. Gui X, Deng M, Song H, Chen Y, Xie J, Li Z *et al*: Disrupting LILRB4/APOE Interaction by an Efficacious Humanized Antibody Reverses T-cell Suppression and Blocks AML Development. *Cancer Immunol Res* 2019, 7(8):1244-1257.
19. Deng M, Gui X, Kim J, Xie L, Chen W, Li Z *et al*: LILRB4 signalling in leukaemia cells mediates T cell suppression and tumour infiltration. *Nature* 2018, 562(7728):605-609.
20. Barkal AA, Weiskopf K, Kao KS, Gordon SR, Rosental B, Yiu YY *et al*: Engagement of MHC class I by the inhibitory receptor LILRB1 suppresses macrophages and is a target of cancer immunotherapy. *Nat Immunol* 2018, 19(1):76-84.
21. Knaus HA, Berglund S, Hackl H, Montiel-Esparza R, Levis MJ, Karp JE *et al*: Acute Myeloid Leukemia (AML) Blasts Influence the Gene Expression Signature and Co-Signaling Receptor Expression of CD8+ T Cells. *Blood* 2016, 128(22):1700-1700.
22. Zheng J, Umikawa M, Cui C, Li J, Chen X, Zhang C *et al*: Inhibitory receptors bind ANGPTLs and support blood stem cells and leukaemia development. *Nature* 2012, 485(7400):656-660.
23. Consortium G: The Genotype-Tissue Expression (GTEx) project. *Nat Genet* 2013, 45(6):580-585.
24. Pontén F, Jirström K, Uhlen M: The Human Protein Atlas--a tool for pathology. *J Pathol* 2008, 216(4):387-393.
25. Barretina J, Caponigro G, Stransky N, Venkatesan K, Margolin AA, Kim S *et al*: The Cancer Cell Line Encyclopedia enables predictive modelling of anticancer drug sensitivity. *Nature* 2012, 483(7391):603-607.
26. Ritchie ME, Phipson B, Wu D, Hu Y, Law CW, Shi W *et al*: limma powers differential expression analyses for RNA-sequencing and microarray studies. *Nucleic Acids Res* 2015, 43(7):e47.
27. Dufva O, Pölönen P, Brück O, Keränen MAI, Klievink J, Mehtonen J *et al*: Immunogenomic Landscape of Hematological Malignancies. *Cancer Cell* 2020, 38(3):380-399.e313.
28. Tyner JW, Tognon CE, Bottomly D, Wilmot B, Kurtz SE, Savage SL *et al*: Functional genomic landscape of acute myeloid leukaemia. *Nature* 2018, 562(7728):526-531.
29. Mayakonda A, Lin DC, Assenov Y, Plass C, Koeffler HP: Maftools: efficient and comprehensive analysis of somatic variants in cancer. *Genome Res* 2018, 28(11):1747-1756.
30. Mermel CH, Schumacher SE, Hill B, Meyerson ML, Beroukhim R, Getz G: GISTIC2.0 facilitates sensitive and confident localization of the targets of focal somatic copy-number alteration in human cancers. *Genome Biol* 2011, 12(4):R41.
31. Liu CJ, Hu FF, Xia MX, Han L, Zhang Q, Guo AY: GSCALite: a web server for gene set cancer analysis. *Bioinformatics* 2018, 34(21):3771-3772.
32. Prange KHM, Mandoli A, Kuznetsova T, Wang SY, Sotoca AM, Marneth AE *et al*: MLL-AF9 and MLL-AF4 oncofusion proteins bind a distinct enhancer repertoire and target the RUNX1 program in 11q23 acute myeloid leukemia. *Oncogene* 2017, 36(23):3346-3356.

33. Li T, Fu J, Zeng Z, Cohen D, Li J, Chen Q *et al*: TIMER2.0 for analysis of tumor-infiltrating immune cells. *Nucleic Acids Res* 2020, 48(W1):W509-W514.
34. Camp RL, Dolled-Filhart M, Rimm DL: X-tile: a new bio-informatics tool for biomarker assessment and outcome-based cut-point optimization. *Clin Cancer Res* 2004, 10(21):7252-7259.
35. Tamborero D, Rubio-Perez C, Muiños F, Sabarinathan R, Piulats JM, Muntasell A *et al*: A Pan-cancer Landscape of Interactions between Solid Tumors and Infiltrating Immune Cell Populations. *Clin Cancer Res* 2018, 24(15):3717-3728.
36. Sturm G, Finotello F, Petitprez F, Zhang JD, Baumbach J, Fridman WH *et al*: Comprehensive evaluation of transcriptome-based cell-type quantification methods for immuno-oncology. *Bioinformatics* 2019, 35(14):i436-i445.
37. De Simone M, Arrigoni A, Rossetti G, Gruarin P, Ranzani V, Politano C *et al*: Transcriptional Landscape of Human Tissue Lymphocytes Unveils Uniqueness of Tumor-Infiltrating T Regulatory Cells. *Immunity* 2016, 45(5):1135-1147.
38. Maag JLV: gganatogram: An R package for modular visualisation of anatograms and tissues based on ggplot2. *F1000Res* 2018, 7:1576.
39. The Genotype-Tissue Expression (GTEx) project. *Nat Genet* 2013, 45(6):580-585.
40. Sun Y, Liu J, Gao P, Wang Y, Liu C: Expression of Ig-like transcript 4 inhibitory receptor in human non-small cell lung cancer. *Chest* 2008, 134(4):783-788.
41. Cheng J, Gao X, Zhang X, Guo H, Chen S, Gou X: Leukocyte immunoglobulin-like receptor subfamily B member 1 potentially acts as a diagnostic and prognostic target in certain subtypes of adenocarcinoma. *Med Hypotheses* 2020, 144:109863.
42. Rapin N, Bagger FO, Jendholm J, Mora-Jensen H, Krogh A, Kohlmann A *et al*: Comparing cancer vs normal gene expression profiles identifies new disease entities and common transcriptional programs in AML patients. *Blood* 2014, 123(6):894-904.
43. Su R, Dong L, Li Y, Gao M, Han L, Wunderlich M *et al*: Targeting FTO Suppresses Cancer Stem Cell Maintenance and Immune Evasion. *Cancer Cell* 2020, 38(1):79-96.e11.
44. Hurtz C, Chan LN, Geng H, Ballabio E, Xiao G, Deb G *et al*: Rationale for targeting BCL6 in MLL-rearranged acute lymphoblastic leukemia. *Genes Dev* 2019, 33(17-18):1265-1279.
45. Akalin A, Garrett-Bakelman FE, Kormaksson M, Busuttil J, Zhang L, Khrebtukova I *et al*: Base-pair resolution DNA methylation sequencing reveals profoundly divergent epigenetic landscapes in acute myeloid leukemia. *PLoS Genet* 2012, 8(6):e1002781.
46. Xu ZJ, Ma JC, Zhou JD, Wen XM, Yao DM, Zhang W *et al*: Reduced protocadherin17 expression in leukemia stem cells: the clinical and biological effect in acute myeloid leukemia. *J Transl Med* 2019, 17(1):102.
47. Sakhdari A, Tang Z, Ok CY, Bueso-Ramos CE, Medeiros LJ, Huh YO: Homogeneously staining region (hsr) on chromosome 11 is highly specific for KMT2A amplification in acute myeloid leukemia (AML) and myelodysplastic syndrome (MDS). *Cancer Genet* 2019, 238:18-22.

48. Peterson JF, Sukov WR, Pitel BA, Smoley SA, Pearce KE, Meyer RG *et al*: Acute leukemias harboring KMT2A/MLLT10 fusion: a 10-year experience from a single genomics laboratory. *Genes Chromosomes Cancer* 2019, 58(8):567-577.
49. John S, Chen H, Deng M, Gui X, Wu G, Chen W *et al*: A Novel Anti-LILRB4 CAR-T Cell for the Treatment of Monocytic AML. *Mol Ther* 2018, 26(10):2487-2495.
50. Liu X, Yu X, Xie J, Zhan M, Yu Z, Xie L *et al*: ANGPTL2/LILRB2 signaling promotes the propagation of lung cancer cells. *Oncotarget* 2015, 6(25):21004-21015.
51. Cheng J, Luan J, Chen P, Kuang X, Jiang P, Zhang R *et al*: Immunosuppressive receptor LILRB1 acts as a potential regulator in hepatocellular carcinoma by integrating with SHP1. *Cancer Biomark* 2020, 28(3):309-319.
52. Uhl FM, Chen S, O'Sullivan D, Edwards-Hicks J, Richter G, Haring E *et al*: Metabolic reprogramming of donor T cells enhances graft-versus-leukemia effects in mice and humans. *Sci Transl Med* 2020, 12(567).
53. Mussai F, De Santo C, Abu-Dayyeh I, Booth S, Quek L, McEwen-Smith RM *et al*: Acute myeloid leukemia creates an arginase-dependent immunosuppressive microenvironment. *Blood* 2013, 122(5):749-758.
54. Curti A, Aluigi M, Pandolfi S, Ferri E, Isidori A, Salvestrini V *et al*: Acute myeloid leukemia cells constitutively express the immunoregulatory enzyme indoleamine 2,3-dioxygenase. *Leukemia* 2007, 21(2):353-355.
55. Tonks A, Hills R, White P, Rosie B, Mills KI, Burnett AK *et al*: CD200 as a prognostic factor in acute myeloid leukaemia. *Leukemia* 2007, 21(3):566-568.
56. Li C, Chen X, Yu X, Zhu Y, Ma C, Xia R *et al*: Tim-3 is highly expressed in T cells in acute myeloid leukemia and associated with clinicopathological prognostic stratification. *Int J Clin Exp Pathol* 2014, 7(10):6880-6888.
57. Perna F, Berman SH, Soni RK, Mansilla-Soto J, Eyquem J, Hamieh M *et al*: Integrating Proteomics and Transcriptomics for Systematic Combinatorial Chimeric Antigen Receptor Therapy of AML. *Cancer Cell* 2017, 32(4):506-519.e505.

Figures

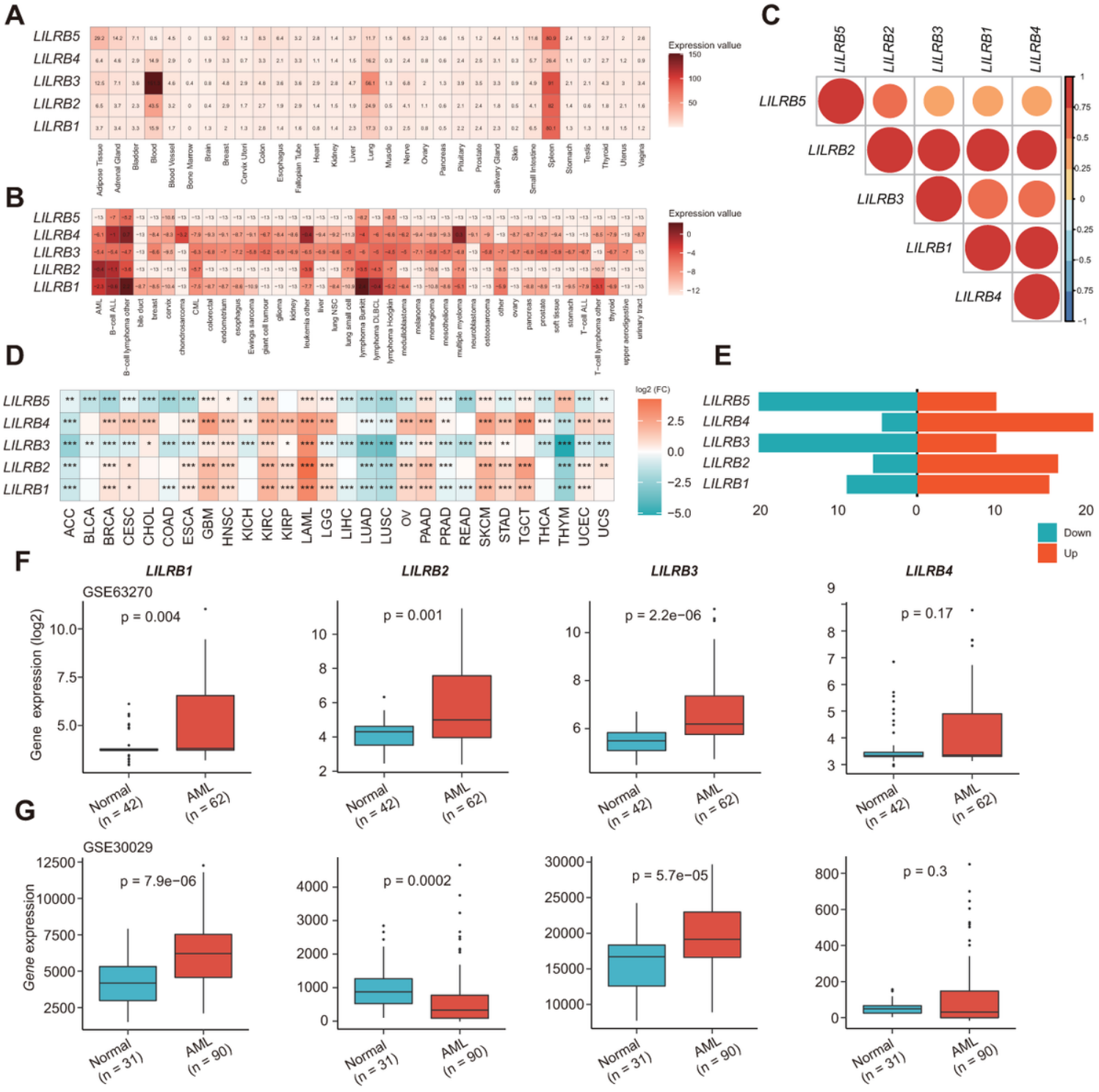

Figure 1

Expression patterns of LILRBs in normal tissues, cancer cell lines, and primary tumor samples. (a) Heatmap showing mRNA expression levels of LILRBs in normal tissues from the Genotype-Tissue Expression (GTEx) database. (b) Heatmap showing mRNA expression levels of LILRBs in various tumor cell lines from the Cancer Cell Line Encyclopedia (CCLE) database. (c) Correlation matrix of the expression of LILRB1-LILRB5 in the TCGA pan-cancer dataset. (d) Heatmap of differential expression profiles of LILRBs between tumor and normal samples, combining data from TCGA and GTEx databases.

The color depicts the log2-transformed fold change (Log2FC) between tumor and normal tissues. *P < 0.05; **P < 0.01; ***P < 0.001. (e) Bar plot showing genes significantly upregulated and downregulated (P < 0.05) across different cancer types. Red, up-regulated expression; blue, down-regulated expression. (f and g) Box plots showing expression levels of LILRB1-4 in normal controls and AML in the GSE63270 (f) and GSE30029 (g) datasets.

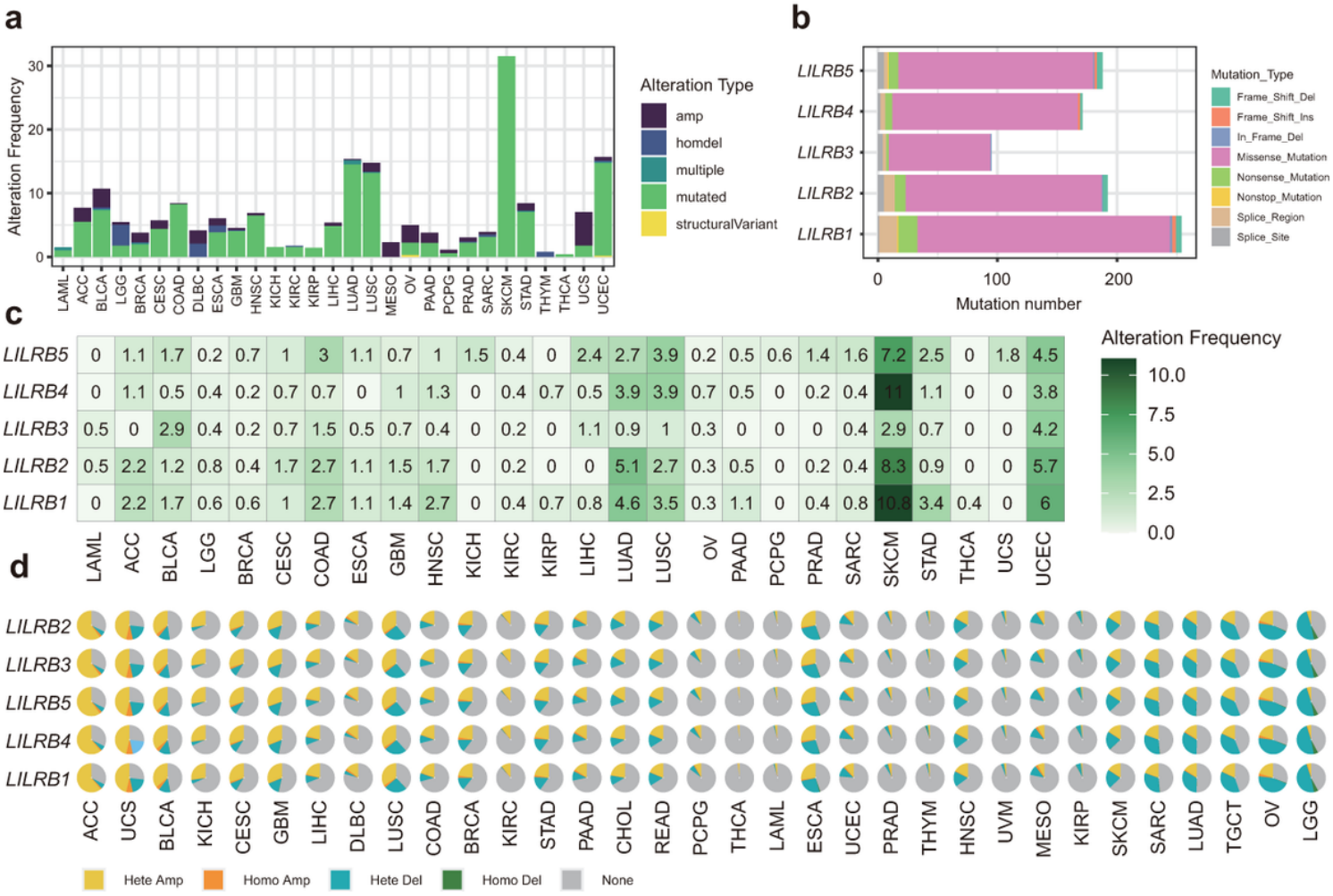

Figure 2

Landscape of genetic alterations of LILRBs in tumors. (a) Genetic alteration frequencies of LILRBs across different tumors from TCGA. (b) Bar plot showing the percentages of various mutation types for five LILRB genes. (c) Heat map showing mutation frequencies of LILRBs across different cancer types. Numbers on the cells represent mutation percentages. (d) Pie plots showing the percentages of various copy number alteration (CNA) types for five LILRB genes.

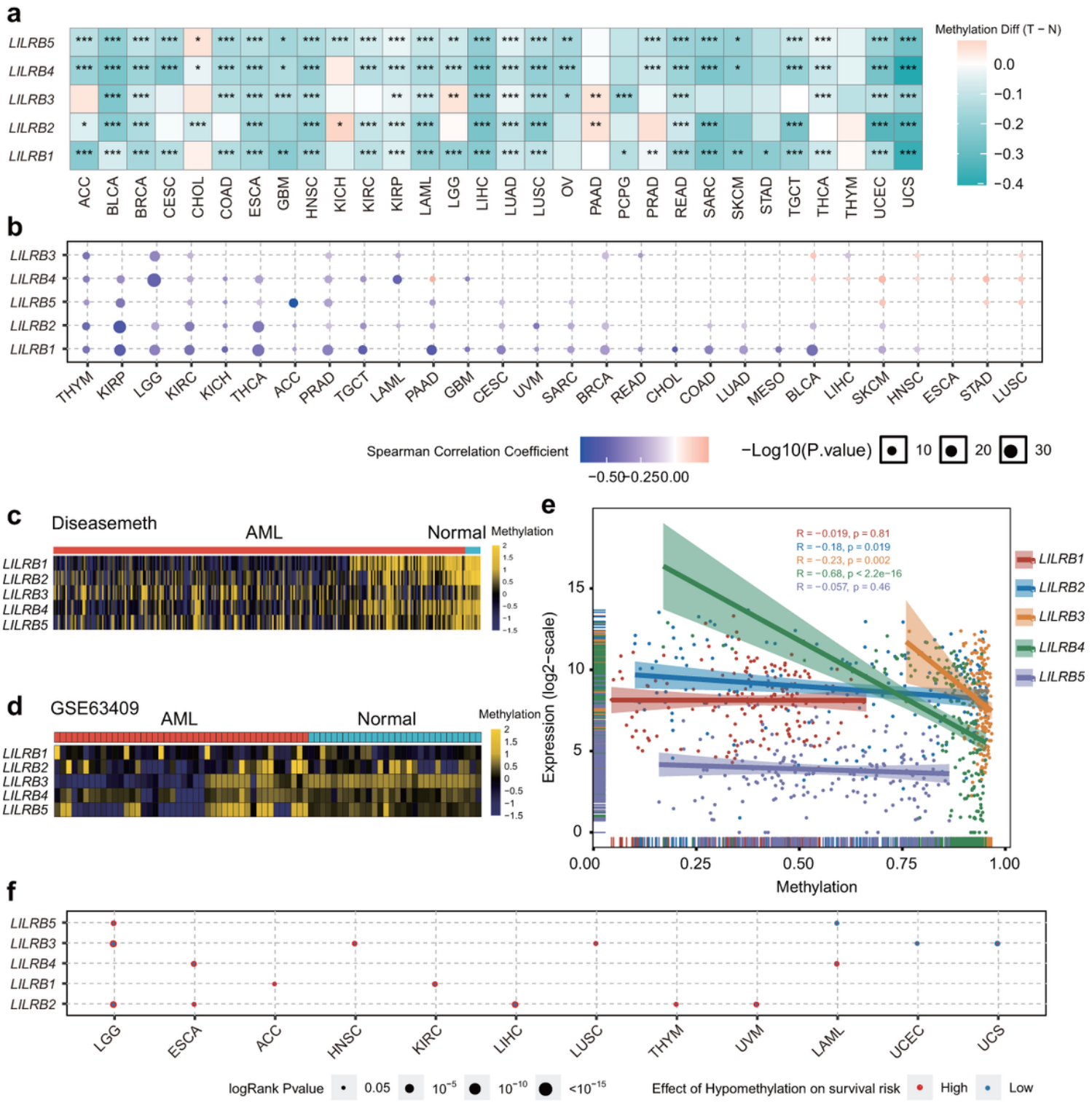

Figure 3

DNA methylation aberration of LILRBs in tumors. (a) Heatmap of differential methylation profiles of LILRBs between tumor and normal samples, using data from the Diseasemeth database. The color depicts methylation differences between tumor (T) and normal (N) tissues. *P < 0.05; **P < 0.01; ***P < 0.001. (b) Correlation between methylation and mRNA expression of LILRBs analyzed via the GSCALite platform. Blue dots indicate negative correlation and red indicate positive correlation. The size of the

point represents the statistical significance. (c and d) Heatmap showing methylation of LILRB genes in the Diseasemeth dataset (AML, n = 271; Normal, n = 10) (c) and the GSE63409 dataset (AML, n = 44; Normal, n = 30) (d). (e) Scatterplot showing the correlation between mRNA expression and DNA methylation levels of LILRBs in the TCGA AML dataset. Spearman correlation coefficients and p-values are indicated. The linear models describing the correlations are depicted as straight lines. The marginal rugs drawn on the axis of the scatter plots were used to show the distributions of two variables. (f) Correlation between LILRBs methylation and survival across cancers analyzed via the GSCALite platform. Red dots indicate a higher risk conveyed by hypomethylation and blue indicate lower risk. The size of the point represents the statistical significance.

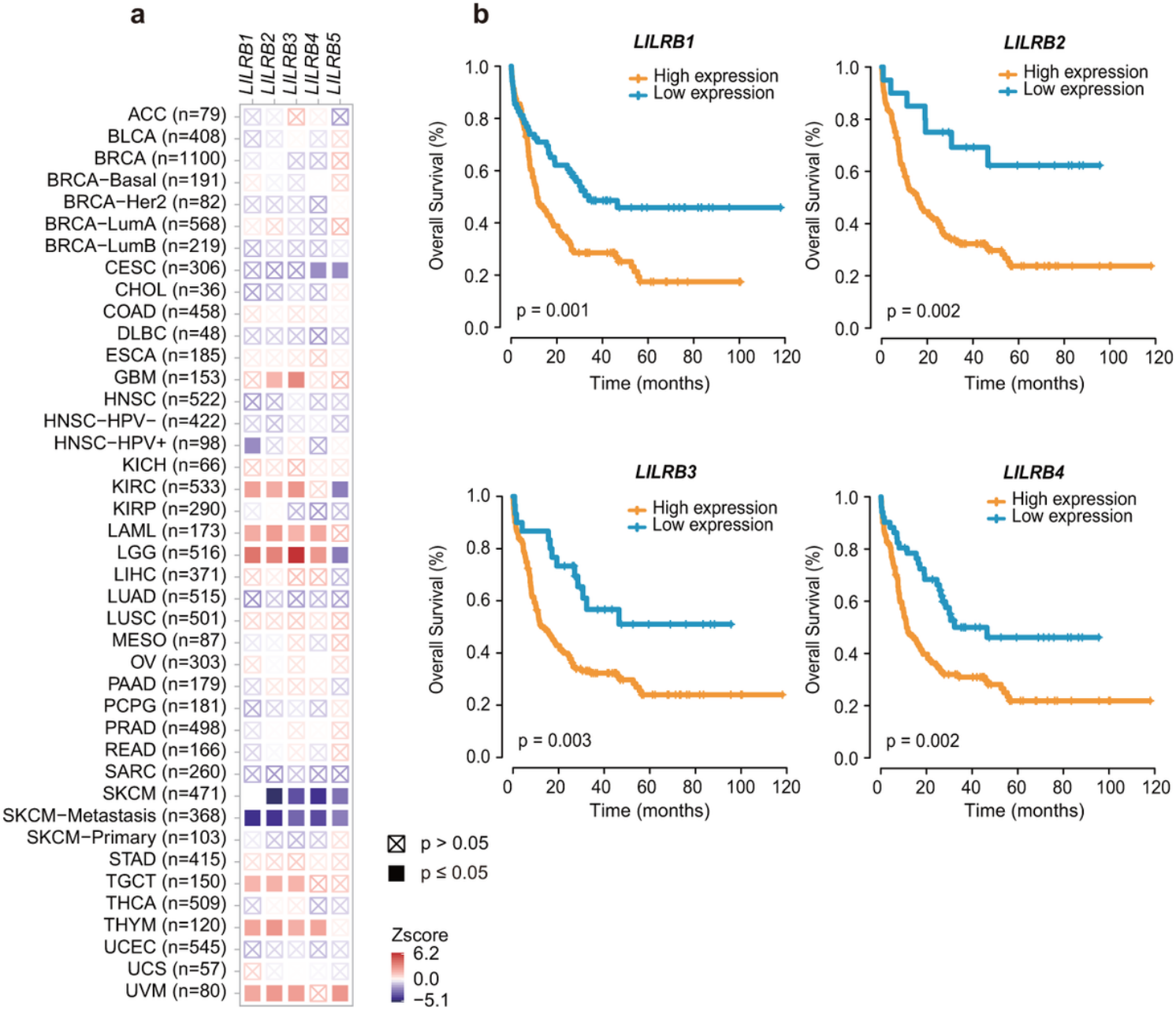

Figure 4

The prognostic impacts of LILRBs in cancers. (a) Association between LILRBs expression and patient prognosis across 33 cancer types as determined by the TIMER2.0 database. (b) Kaplan-Meier curves representing OS of AML patients from the TCGA cohort based on the expression of indicated LILRB members (LILRB1-LILRB4).

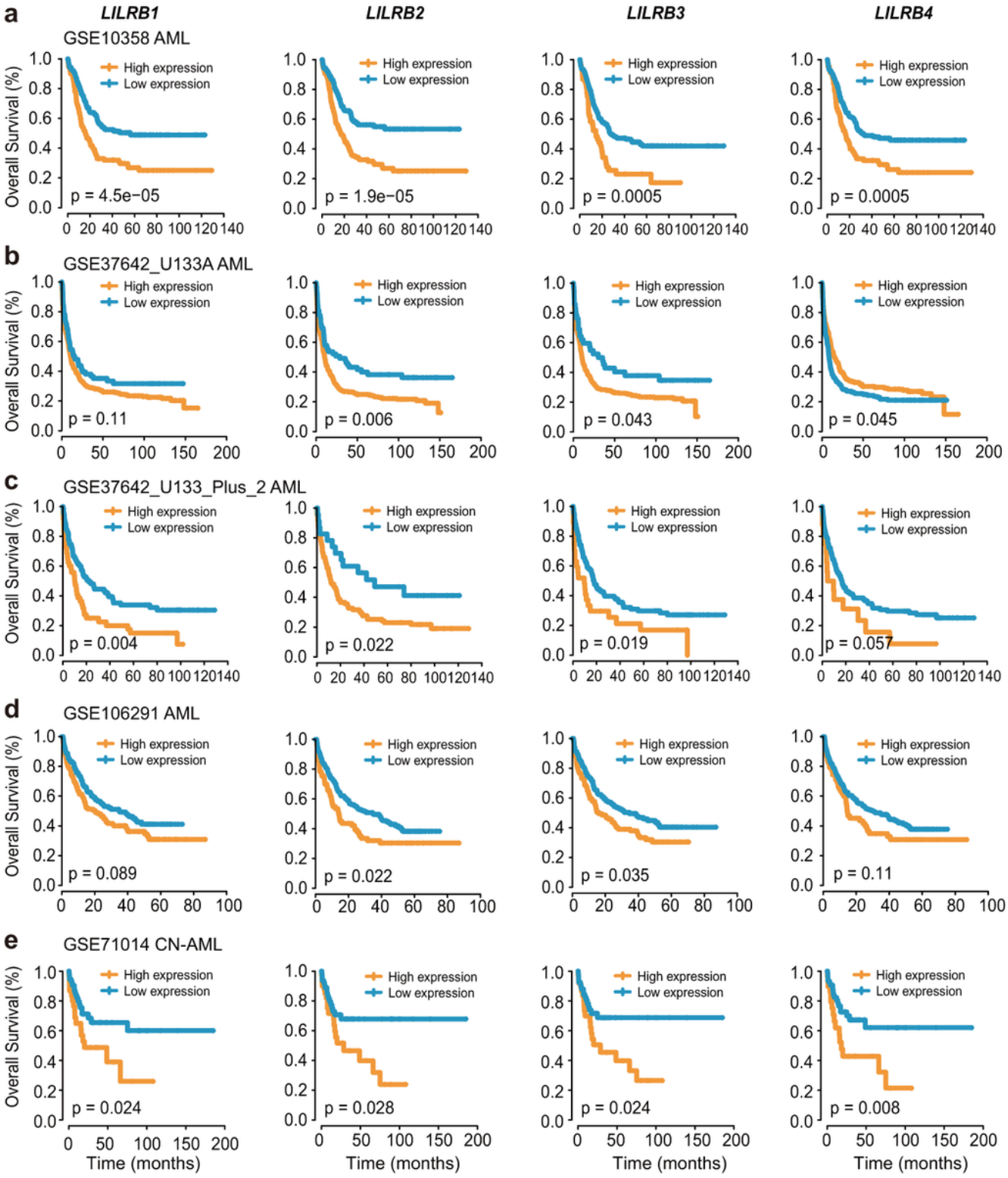

Figure 5

Independent validation of the prognostic significance of LILRBs in five GEO datasets. (a-e) Kaplan-Meier curves representing OS of five AML cohorts from GEO (GSE10358, n = 304; GSE37642 [U133A], n = 422; GSE37642 [U133plus2], n = 140; GSE106291, n = 250; GSE71014, n = 104) based on the expression of indicated LILRB members (LILRB1-LILRB4).

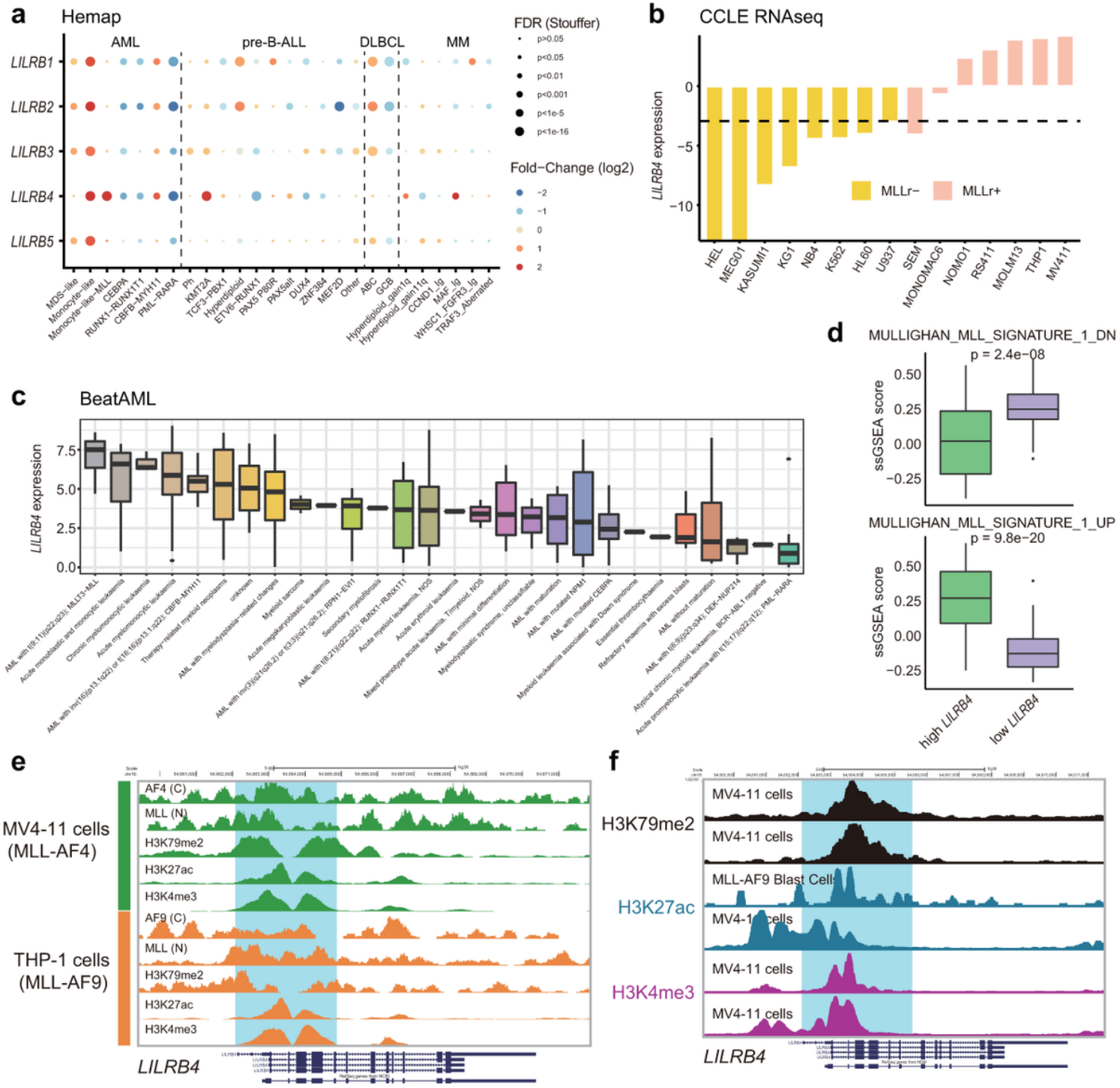

Figure 6

LILRB4 is aberrantly overexpressed in MLL-rearranged AML and is likely a direct target of MLL-fusion proteins. (a) Expression differences of LILRB genes in molecular subtypes of AML, and pre-B-ALL, DLBCL, and MM. The expression fold change between each subtype and the remaining samples in the same

disease were compared using the Wilcoxon rank sum test. The color of the dots indicates fold changes (log2) and size indicates the FDR values. The FDR values were categorized into five groups based on significance cutoffs for visualization (0.05, 0.01, 0.001, 1e-5, 1e-16). (b) Bar plot showing LIRB4 expression (RNA-seq) in non-MLL-rearranged (HEL, MEG01, KASUMI1, KG1, NB4, K562, HL60, U937) and MLL-rearranged (SEM, MONOMAC6, NOMO1, RS411, MOLM13, THP1, MV411) cell lines from the CCLE database. The dotted line represents the mean expression of LILRB4 across all cell lines analyzed. (c) Comparison of LILRB4 expression among human primary AML cases with MLL rearrangements and those without MLL rearrangements in the BeatAML dataset. (d) Box plots showing ssGSEA scores of two MLL-related gene signatures (MULLIGHAN_MLL_SIGNATURE_1_DN and MULLIGHAN_MLL_SIGNATURE_1_UP) between patients (TCGA dataset) with high and low LILRB4 expression. (e) ChIP-seq tracks for MLL-fusion proteins, H3K79me2, H3K27ac, and H3K4me3 at LILRB4 gene loci in MV4-11 and THP-1 cell lines. ChIP-seq data were obtained from GSE79899. (f) ChIP-seq tracks for H3K79me2, H3K27ac, and H3K4me3 at LILRB4 gene loci in MV4-11 and MLL-AF9 transformed blast cells. ChIP-seq data were obtained from GSE82116, GSE71779, GSE89336, GSE71776, and GSE61785.

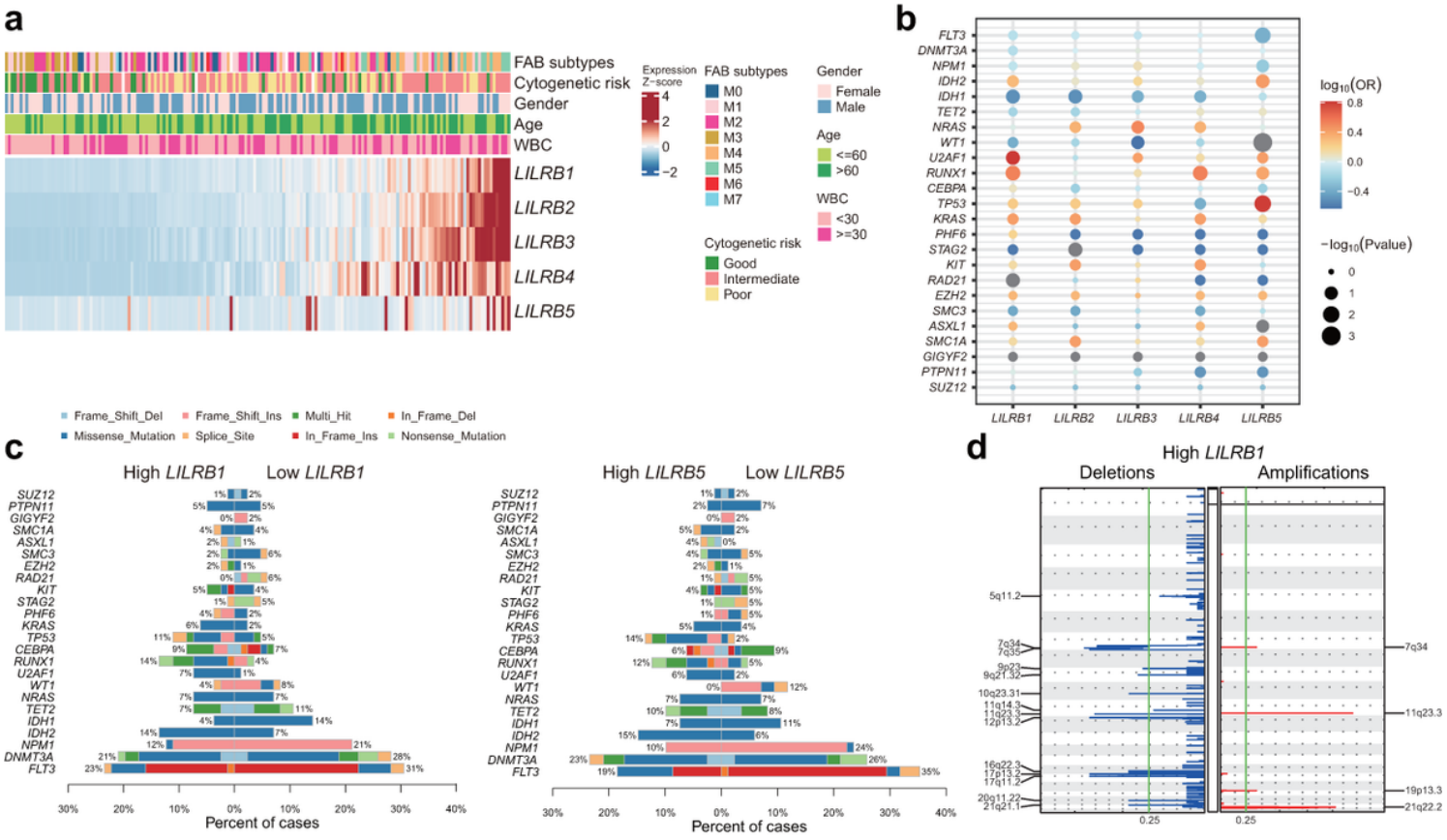

Figure 7

LILRBs expression correlate with distinct genomic alterations in AML. (a) Heatmap showing association between LILRBs expression and clinical characteristics in the TCGA AML cohort. (b) Bubble plot showing associations between the expression of LILRB1-LILRB5 and common mutational events in the TCGA dataset. Bubble size indicates −log10 (Fisher test p-value). Color signifies −log10 (odds ratio), positive

association is indicated with red circles, negative with blue circles, and non-association with gray circles. (c) Co-bar plots showing the comparison of mutational profiles between patients with high and low LILRB1/LILRB5 expression in the TCGA dataset. (d) GISTIC analyses identified recurrent copy number alterations in AML patients with high LILRB1 expression.

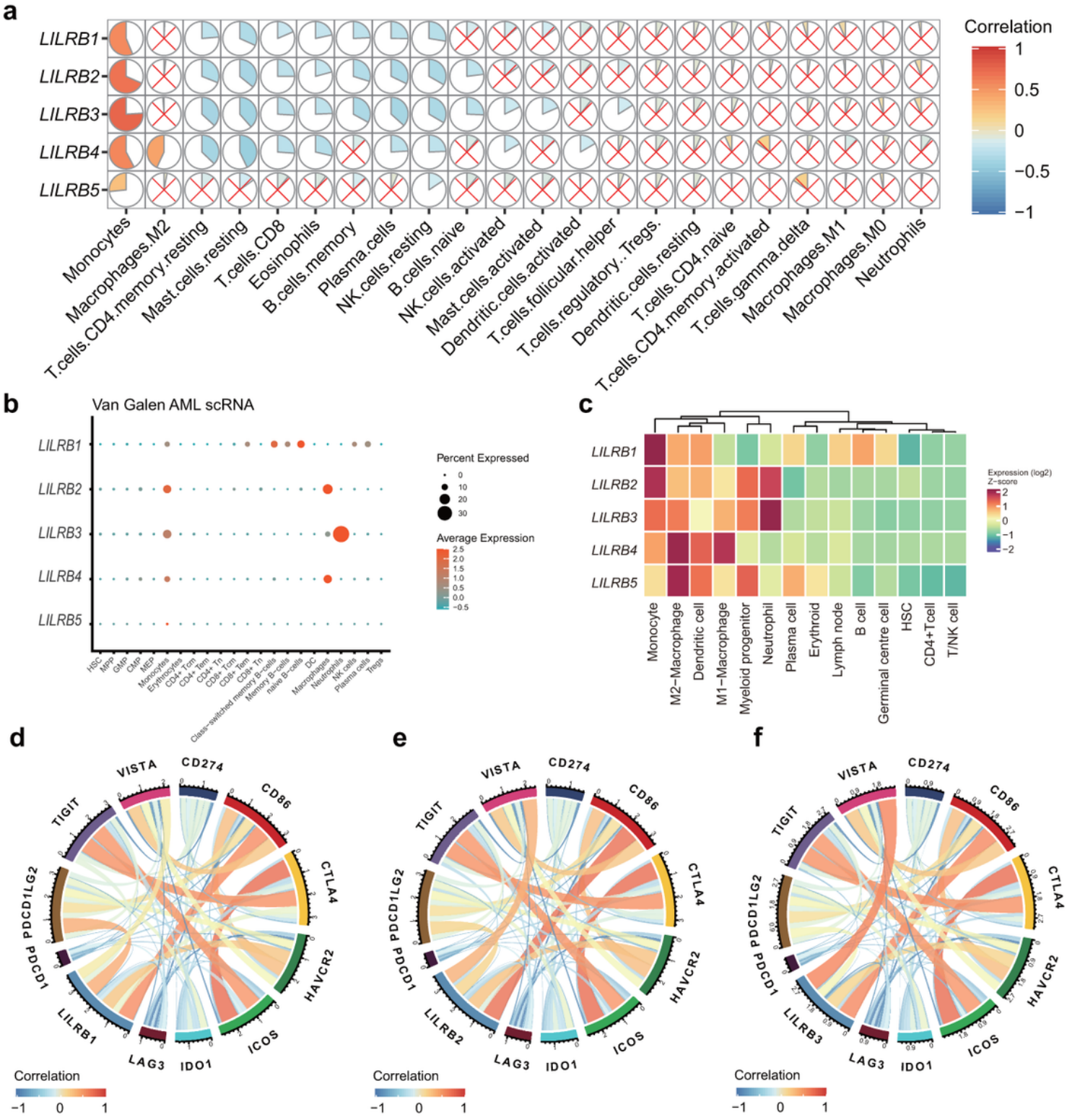

Figure 8

The relation between LILRBs expression with immune cell infiltration and immune checkpoints. (a) Correlation matrix plot showing correlations between LILRBs and tumor immune infiltrating cells (TIICs). The overall immune cell compositions were estimated by CIBERSORT in the TCGA dataset. (b) Dot plot showing expression pattens of LILRBs in annotated cell types from 16 AML scRNA-seq samples (Van Galen AML scRNA). The color of the dots indicates average expression and size indicates percentage of cells with detectable expression. (c) Heatmap showing LILRBs expression in normal cell populations from the Hemap dataset. (d-f) Circos plots showing correlation between the expression of LILRB1 (d), LILRB2 (e), and LILRB3 (f) and immune checkpoint genes in the TCGA dataset.

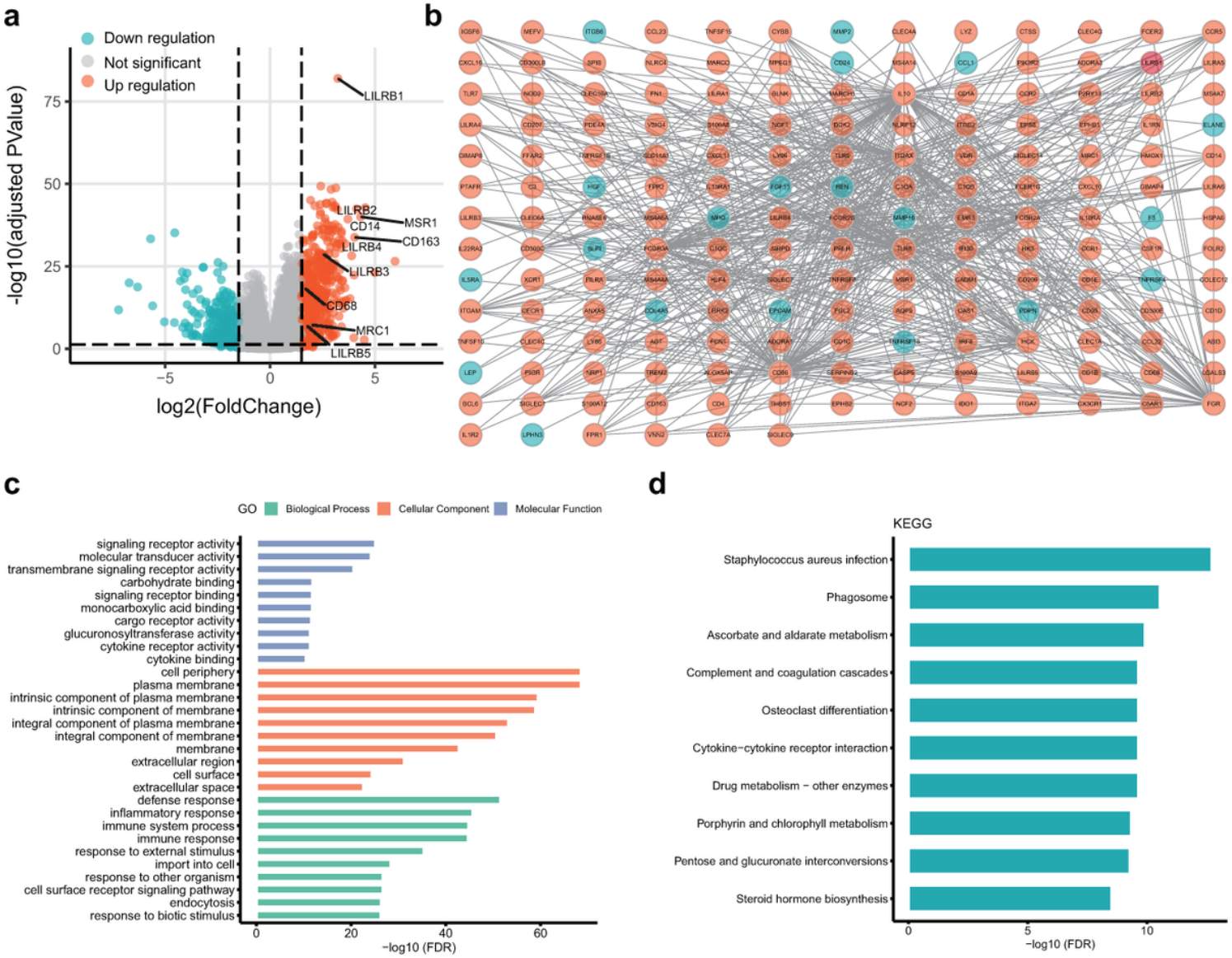

Figure 9

The biological significance of LILRBs expression in AML. (a) Volcano plot showing differentially expressed genes (DEGs) between high and low LILRB1 expressers. (b) Cytoscape analysis of LILRB1-related network using PPI information obtained from STRING database (http://stringdb.org/). Red nodes represent up-regulated genes and blue represent down-regulated genes. (c and d) GO (c) and KEGG (d) analysis of DEGs.

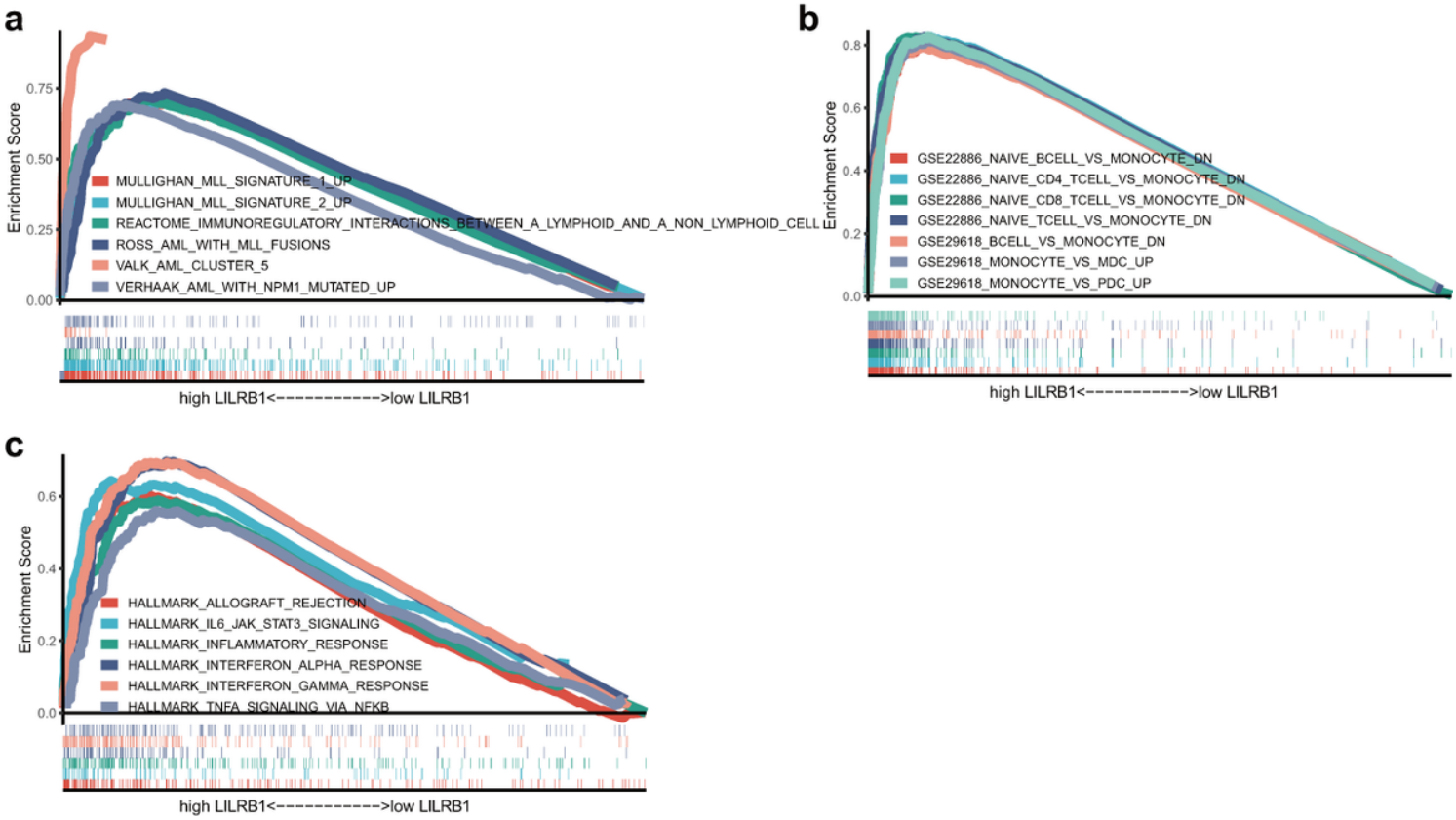

Figure 10

Gene set enrichment analysis (GSEA) of patients with high and low LILRB1 expression, with curated (a), immunologic (b), and hallmark (c) gene sets obtained from the Molecular Signatures Database (MSigDB).

Supplementary Files

This is a list of supplementary files associated with this preprint. Click to download.

- SupplementaryData1.xlsx
- SupplementaryData2.xlsx
- SupplementaryData3.xlsx
- SupplementaryInformation.docx